# The biocompatibility of bone cements: progress in methodological approach

**Carlo Dall'Oca,[1] Tommaso Maluta,[1] Gian Mario Micheloni,[1] Matteo Cengarle,[1] Giampaolo Morbioli,[2] Paolo Bernardi,[3] Andrea Sbarbati,[3] Daniele Degl'Innocenti,[3] Franco Lavini,[1] Bruno Magnan[1]**

**[1]Department of Surgery, Orthopaedic and Traumatology Clinic, University of Verona**
**[2]CIRSAL - Interdepartmental Center of Scientific Research on Laboratory Animals, University of Verona**
**[3]Department of Neuroscience, Biomedicine and Movement, Human Anatomy and Histology Section, University of Verona, Italy**

## Abstract

The ideal bone graft substitute should have certain properties and there are many studies dealing with mixture of polymethylmetacrilate (PMMA) and β-tricalciumphospate (β-TCP) presenting the best characteristics of both. Scanning Electron Microscopy (SEM), for ultra-structural data, resulted a very reliable *in vivo* model to better understand the bioactivity of a cement and to properly evaluate its suitability for a particular purpose. The present study aims to further improve the knowledge on osteointegration development, using both parameters obtained with the Environmental Scanning Electron Microscopy (ESEM) and focused histological examination. Two hybrid bone graft substitute were designed among ceramic and polymer-based bone graft substitutes. Based on β-TCP granules sizes, they were created with theoretical different osteoconductive properties. An acrylic standard cement was chosen as control. Cements were implanted in twelve New Zealand White (NZW) rabbits, which were sacrificed at 1, 2, 3, 6, 9 and 12 months after cement implantation. Histological samples were prepared with an infiltration process of LR white resin and then specimens were studied by X-rays, histology and Environmental Scanning Electron Microscopy (ESEM). Comparing the resulting data, it was possible to follow osteointegration's various developments resulting from different sizes of β-TCP granules. In this paper, we show that this evaluation process, together with ESEM, provides further important information that allows to follow any osteointegration at every stage of develop.

## Introduction

More than 500,000 bone grafting procedures are performed yearly in the United States, to fill bone defects in orthopaedic surgery, neurosurgery and dentistry.[1,2] Bone graft is the second most common transplantation tissue, with blood being by far the commonest.[3] Bone graft substitutes can either replace autologous bone graft or expand an existing amount of autologous bone graft. Autologous bone remains the gold standard for stimulating bone repair and regeneration. However there are several limitations, especially if there is massive segmental bone loss or a very large cancellous void.[4] The ideal bone graft substitute should be biocompatible, bioabsorbable, osteoconductive, osteoinductive, structurally similar to the bone, easy to use and cost effective.[5,6] There are many studies dealing with mixture of polymethylmetacrilate (PMMA) and β-tricalciumphospate (β-TCP) and presenting the best bone graft substitution characteristics of both.[7-9] In fact, β-TCPs are reabsorbed through cell-mediated processes, including osteoclast activity.[10,11] As a consequence of this mechanism resembling bone remodelling, β-TCP will not disappear until new bone is being formed.[12] Therefore by mixing PMMA and β-TCP, a bone void filler can be created with osteoconductive properties i.e. properties of bioactivity.[13,14] In this case bioactivity, as the interaction between a biomaterial and the surrounding tissue, describes the influence of a material on bone formation.[13,15-17] To better understand the bioactivity of a cement and to properly evaluate the suitability of cements for a particular purpose, Dall'Oca *et al*.[13] have demonstrated the usefulness of the ultrastructural data obtained by Scanning Electron Microscopy (SEM) and proposed a new procedure to test the bioactivity of acrilic cements *in vivo* models. This approach improves the visualization of the bone-cement interface, adding new data on the behavior of an important component of treatment.[13] Porous cements made of β-TCP/PMMA could be considered for vertebroplastic or augmentation orthopaedics uses,[14,18-20] but further studies are necessary in order to evaluate the *in vivo* properties of this material. The present study aims to further improve the proposed procedure, using parameters obtained with the Environmental Scanning Electron Microscopy (ESEM).

Correspondence: Carlo Dall'Oca, Department of Surgery, Orthopaedic and Traumatology Clinic, University of Verona, Ospedale Borgo Trento, Piazzale A. Stefani 1, 37126 Verona, Italy.
Tel. +39.045.8123542 - Fax: +39.045.8027470.
E-mail: carlo.dalloca@univr.it

Key words: Plymethylmetacrilate; calcium phosphate cement; osteointegration; biocompatibility; Environmental Scanning Electron Microscopy.

Acknowledgments: we thank the company Tecres S.p.A., Sommacampagna, VR, Italy, for providing the cements used in this trial.

Received for publication: 28 April 2016.
Accepted for publication: 7 March 2017.


*European Journal of Histochemistry 2017; 61:2673*
*doi:10.4081/ejh.2017.2673*

## Materials and Methods

### Bone cements

A hybrid bone graft substitute was designed between ceramic and polymer-based bone graft substitutes. It is made up of a mixture of PMMA and β-TCP to be osteoconductive, to facilitate osteointegration of the bone void filler. By mixing PMMA with granules and powder of β-TCP, bone void fillers with different osteoconductive properties were created. Pores give bone the opportunity to grow in, resulting in better fixation of the void filler which remains implanted permanently. For control group it was used a PMMA cement without β-TCP(Mendec Spine® Tecres SpA, Sommacampagna, VR, Italy), named C cement. For the experimental groups, two cements presenting different characteristics of porosity were realized, with the purpose of studying the behavior of bone tissue along the time. One using β-TCP in powder (granules of 53 μg) named P cement (Porosectan® I, Tecres SpA) and the second one composed by β-TCP in powder (granules of 53 μg) and granules (100-300 μg), named PG cement (Porosectan® II, Tecres SpA). The β-TCP powder used in this cement meets the medical grade standard

described by ASTM 1088 4a (2010) "Standard Specification for Beta-Tricalcium Phosphate for Surgical Implantation". This was carefully chosen to be aligned with available studies on pore size.[21] The specimens of the implanted material, supplied by the Company Tecres SpA, were made up of cylinders of 2 mm in diameter and 6 mm in length; their composition is shown in Table 1.

All experiments were performed according to the following standards:
UNI EN ISO 10993-6 :2007: *Test of local effects after implantation*;
UNI EN ISO 10993-1 :2004: *Biological evaluation of medical devices. Part 1 Evaluations and testing*;
UNI EN ISO 10993-12 :2005: *Sample and reference materials*.

## Animals

Cements were implanted in twelve New Zealand White (NZW) rabbits, which were sacrificed at 1, 2, 3, 6, 9 and 12 months after implantation of the cement. The animals used were female rabbits weighting between 3 and 4.5 kg before the beginning of the study. The rabbits were reared and operated at CIRSAL (Centro Interdipartimentale per la Ricerca Scientifica su Animali da Laboratorio - Interdepartmental Center of Scientific Research on Laboratory Animals, University of Verona). Breeding conditions were in accordance with the European Directives (CE Directive 86/609) and UNI EN ISO 10993-2; (2006): *Animal welfare requirement*. They were bred in an individual metallic cage (Tecniplast® according to D.Lgs 116/02) and fed with complete granular diet for rabbits, *ad libitum*. Water was freely accessible. Temperature was between 15 to 21°C and room relative humidity was between 30% to 70%. The operative staff was qualified and educated. Experiments were approved by Ethics Committee of Verona University and performed in accordance with the Guideline for Animal Experimentation of the Italian Department of Health, under the supervision of a veterinarian, and organized to minimize stress and the number of rabbits used.

## Surgery

After trichotomy of concerned area, each rabbit was brought into operatory room and positioned lateral on the operatory table. General anesthesia induction was carried out by a veterinarian with intramuscular injection of an association of tiletamine hydrochloride and zolazepam hydrochloride (Zoletil 100®) at a dose of 20 mg/kg and Xylazione (Rompun®) at a dose of 5 mg/kKg. A local anesthesia with lidocaine was also injected in the site of the surgical incision.

After washing, disinfection and preparation of sterile operatory field, we made small skin incisions on lateral surface of both femur. The femur was drilled with sterile electrical drill (diameter 2 mm, depth 6 mm), in femoral distal and proximal metaphysis on the right femur and in proximal metaphysis on the left one. After drilling, we washed and cleaned the holes to remove every bone fragments created. We filled the femoral cavities with cement cylinders, in particular P cement distally and PG cement proximally in the right femur, C cement in the proximal methaphysys of the left femur. We did skin suture with not reabsorbable spin Prolene® n. 3-0. After final disinfection, we made an elastic adhesive bandage. Analgesic therapy with Altadol® IM (4 mg/Kg) was administrated to the rabbits, after that the animals were located under UV lamp for ten minutes, before returns in their cage.

## Post-operative clinical follow-up and animal sacrifice

Animals were observed daily to detect clinical abnormalities and antibiotic therapy was administrated for four days (Baytril® 2.5% SC 5 mg/Kg). Medications with iodate antiseptic (Braunol®) were done, and cutaneous stitches were removed 10 days after surgery. The rabbits' state of well-being was assessed with physiological elements (feeding, stool and urine), physical elements (functions of operated limb and coat growth) and behavior elements, like "open field". This test, known as "escape test", is an indication of fear response (rabbit is prey animal, with avoidance reactions, like fear of new situations and human presence).

Rabbits were sacrificed through pharmacology euthanasia with a lethal injection of Tanax® after 1-2-3-6-9-12 months. Both femurs were extracted from thigh, bone curettage from soft tissues was carried out and then all bones were put inside a transparent sterile envelope.

## Macroscopic and radiographic examination, MRI observation

After the removal of the femurs, macroscopic observations and digital pictures of the implant areas were performed. A radiographic examination was carried out *post mortem* using a Philips Practix 360 mobile radiography system, to define the area of samples: it consisted of antero-posterior and lateral side of left and right femur of each rabbit.

Magnetic resonance imaging (MRI) was acquired the using a Bruker BioSpec tomograph for animals (4.7 T), equipped with self-shielded gradients and BGA9 BGA20 (Bruker, Bremen, Germany). The bones were positioned above the coil flat surface and then into the magnet. T1w and T2w sequences were acquired respectively with techniques Spin Echo and RARE (Rapid Acquisition with Relaxation Enhancement). The acquisition and geometric parameters (number of virtual slices, slice thickness, field of view, the matrix) have been optimized for the bone tissue.

## Histological samples preparation

The freshly explanted femurs were cleaned from soft tissue and rinsed in saline solution, then fixed in buffered formaldehyde (pH=7) for a minimum time of 20 days at 4°C. With reference to the analysis of X-ray and MRI, it was possible to accurately dissect the femur close to the cement cylinders. Each section was progressively

**Table 1. Tested bone cements composition.**

| | C cement | P cement* | PG cement° |
|---|---|---|---|
| Cylinder composition | Polymethylmethacrylate 67.5%<br>Barium sulphate[♯] 30.0%<br>Benzoyl peroxide 2.5% | Polymethylmethacrylate 52.9%<br>β-tricalcium phosphate[§] 26.1%<br>Barium sulphate^ 7.0%<br>Benzoyl peroxide 1.0%<br>Saline solution 13.0% | Polymethylmethacrylate 40.7%<br>β-tricalcium phosphate[§] 33.3%<br>β-tricalcium phosphate granule[$] 8.3%<br>Benzoyl peroxide 1.0%<br>Saline solution 16.7% |

*No granule of β-tricalcium phosphate, only powder; °with granule and powder of β-tricalcium phosphate; [♯]barium sulphate powder; [§]β-tricalcium phosphate powder 53 micron; ^barium bulphate granule 200-400 micron; [$]β-tricalcium phosphate granule 100-300 micron.

dehydrated by immersion in increasing concentrations of ethanol (30%, 50%, 80%, 95%, 100%), leaving the sample steeped for at least 48 h for each concentration, and performing three passages in absolute ethanol. The infiltration with LR white resin was performed at room temperature with 3 passages, each of 72 h, in oxygen-poor environment by placing the samples under vacuum (with glass bell) to promote the penetration of the resins. Polymerization took place by UV radiation at room temperature for at least 3 days in oxygen-poor environment. Once cured, specimens were sectioned with a diamond saw blade mounted on a Leitz microtome according to a plane perpendicular to the femur axis. For each sample, sections were obtained with a thickness of about 100 micron, then manually thinned down to a thickness of 30 µm ±10 with fine abrasive paper (P paper waterproof 1000 WSC BMA) immersed in cold water at 4° C approximately to prevent surface overheating. The obtained sections were stained by immersion in a toluidine blue 1% solution for 5 min, rinsed in running water, immersed in a fuchsine acid 2% solution for 3-5min, rinsed in running water, immersed in a 0.02% solution of acetic acid for 1 minute, stained with fast green (Diapath) for 5 min and finally rinsed. The stained sections were put on slides holders with aqueous upright and observed under an optical microscope Olympus BX51 both bright field and in fluorescence. The digital images were acquired with high resolution camera Quicam connected to Dell PC using software image analysis Imageproplus v.7 (MediaCybernetic, Bethesda, MD, USA).

**Evaluations of biocompatibility (local tolerance) and osteointegration**

The local tolerance was evaluated according to microscopic criteria. A semi-quantitative analysis was defined in accordance with the UNI EN ISO 10993-6:2009. Particular attention was given to the inflammatory response, the behavior of the bone and the nature of the contact bone/implant. Each parameter was evaluated by scoring from 0 (absent) to 4 (severe) allowing an accurate assessment of the phenomena of inflammation and/or foreign body reaction, bone repair and degradation of the material. The biocompatibility evaluation scale is reported in Table 2. To evaluate the osteointegration of the cements, we defined a scale of evidences according to the grading described in Table 3.

### Ultrastructural analysis

In order to obtain samples for the investigation with the ESEM, longitudinal cuts have been performed until the exposure of the surfaces of the plants grafted. In order to better understand the phenomenon of osteointegration, we proceeded to the observation with electron microscope ESEM equipped with Energy Dispersive Spectrometry (EDS) microanalytical Probe. The combined use of ESEM with EDS allows to provide the chemical composition of a point of interest on the sample surface (microanalysis). The sections obtained, with a thickness of about 2-3 mm, were put on aluminum stubs with sticky carbon and observed with the electron microscope ESEM XL 30 FEI Philips low vacuum equipped with EDAX® probe for microanalysis.

## Results

### Post-operative clinical follow-up

The surgery procedure was well-tolerated and the animals managed to feed himself since the day after the operation. Within a few days, they managed to move again inside the cage. Neither signs of local swelling or inflammation, nor systemic signs of cement-toxicity or allergic reactions were found. All the animals subjected to the operation survived.

**Table 2. Biocompatibility evaluation scale.**

| Cell reaction | Definitions | | | | |
|---|---|---|---|---|---|
| Score | 0 | 1 | 2 | 3 | 4 |
| Flogosis | Absent | Slight | Moderate | Intense | Severe |
| Polymorphonuclear cells | 0 | Rare, 1-5 / phf | 5-10 / phf | Intense infiltration | Full |
| Lymphocytes | 0 | Rare, 1-5 / phf | 5-10 / phf | Intense infiltration | Full |
| Plasmacells | 0 | Rare, 1-5 / phf | 5-10 / phf | Intense infiltration | Full |
| Macrophages | 0 | Rare, 1-5 / phf | 5-10 / phf | Intense infiltration | Full |
| Giant cells | 0 | Rare, 1-2 / phf | 3-5 / phf | Intense infiltration | Laminae |
| Necrosis | Absent | Minimum | Slight | Moderate | Severe |
| Neovascularization | Absent | Minimum capillary vessels proliferation, focal, 1-3 bud | Groups of 4-7 capillary vessels with fibroclastic structure of support of support | Wide band of capillary vessels with fibroclastic structure Wide band of capillary vessels with fibroclastic structure of support | |
| Fibrosis | Absent | Thin band | Moderately thick band | Thick band | Thick band |
| Fat infiltration | Absent | Minimum amount of fat associated with fibrosis | Several layers of fat and fibrosis | Stretched and wide accumulation of fat cells around the implant | Wide accumulation of fat completely surrounds the implant |
| Evaluation criteria | Score | Irritation degree | | | |
| | 0.0 – 2.9 | Not irritating | | | |
| | 3.0 – 8.9 | Slightly irritating | | | |
| | 9.0 – 15 | Moderately irritating | | | |
| | > 15 | Severely irritating | | | |

### Macroscopic and radiographic examination, MRI observation

The visual appearance of implants had three kinds of features: some with an evident trace of the plant (Figure 1A), some with a bulge as a consequence of bone callus (Figure 1B) and others with an homogeneous surface where the implant was not identifiable (Figure 1C). These different visual appearances were detected in all three types of cements and in every period without any relationship between the macroscopic and the microscopic findings.

Radiographic analysis (Figure 2) showed a good adjustment and maintenance of the samples in the original implant areas, in all different times and for all three types of cements. In the samples of the PG cement, x-ray images showed a weaker signal compared to C and P cements. In particular, for PG cement the radiographic images at 6 months do not show sufficiently the implant. Because of that a more efficient identification was carried out by magnetic resonance imaging. With the MRI, the implant of the PG cement at 6 months was evident in its shape and position (Figure 3). Newetheless, it was well visible at 12 months (Figure 2I).

### Evaluations of biocompatibility (local tolerance) and usteointegration

The results of the semi-quantitative evaluation of local tolerance (biocompatibility) are reported in Table 4. In the early times (1st month) at the periphery of the implants the formation of a bony capsule of variable thickness is visible. In these areas there are aspects of cellular suffering of

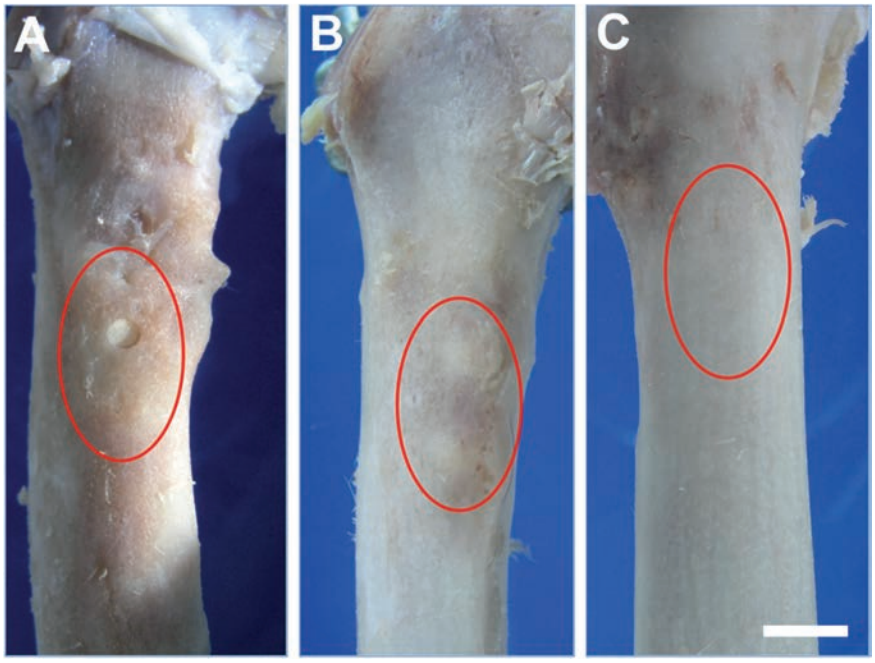


**Figure 1. Macroscopic images of some femurs. Visual appearance of implants: evident trace of the implant (A), bulges resulting in bone callus (B) and implant with external homogenous surface (C). Scale bar: 1 cm.**

**Table 3. Description of grading.**

| Grading | Description |
|---|---|
| G0 | No penetration of organic material inside the resin. |
| G1 | Presence of organic material fuchsin positive into part of the sample |
| G2 | Presence of organic material fuchsin positive in most of the sample |
| G3 | Presence of cells in part of the sample |
| G4 | Presence of cells in the majority of the sample |
| G5 | Presence of osteoid formations within the sample |
| G6 | Training osteonic spread over the whole sample |

**Table 4. Biocompatibility evaluation results.**

| | Score | | | | | | | | | | | | | | | | | |
|---|---|---|---|---|---|---|---|---|---|---|---|---|---|---|---|---|---|---|
| | Month 1 | | | Month 2 | | | Month 3 | | | Month 6 | | | Month 9 | | | Month 12 | | |
| Cement | C | P | PG | C | P | PG | C | P | PG | C | P | PG | C | P | PG | C | P | PG |
| Flogosis | 1 | 0 | 0 | 0 | 0 | 0 | 0 | 0 | 0 | 0 | 0 | 0 | 0 | 0 | 0 | 0 | 0 | 0 |
| Polymorphonuclear cells | 0 | 0 | 0 | 0 | 0 | 0 | 0 | 0 | 0 | 0 | 0 | 0 | 0 | 0 | 0 | 0 | 0 | 0 |
| Lymphocytes | 0 | 0 | 0 | 0 | 0 | 0 | 0 | 0 | 0 | 0 | 0 | 0 | 0 | 0 | 0 | 0 | 0 | 0 |
| Plasmacells | 0 | 0 | 0 | 0 | 0 | 0 | 0 | 0 | 0 | 0 | 0 | 0 | 0 | 0 | 0 | 0 | 0 | 0 |
| Macrophages | 0 | 0 | 0 | 0 | 0 | 0 | 0 | 0 | 0 | 0 | 0 | 0 | 0 | 0 | 0 | 0 | 0 | 0 |
| Giant cells | 0 | 0 | 0 | 0 | 0 | 0 | 0 | 0 | 0 | 0 | 0 | 0 | 0 | 0 | 0 | 0 | 0 | 0 |
| Necrosis | 2 | 2 | 2 | 1 | 1 | 1 | 0 | 0 | 0 | 0 | 0 | 0 | 0 | 0 | 0 | 0 | 0 | 0 |
| Neovascularization | 0 | 0 | 0 | 0 | 0 | 0 | 0 | 0 | 0 | 0 | 0 | 0 | 0 | 0 | 0 | 0 | 0 | 0 |
| Fibrosis | 2 | 2 | 2 | 1 | 2 | 2 | 2 | 2 | 2 | 2 | 2 | 2 | 2 | 2 | 2 | 2 | 2 | 2 |
| Fat infiltration | 0 | 0 | 0 | 0 | 0 | 0 | 0 | 0 | 0 | 0 | 0 | 0 | 0 | 0 | 0 | 0 | 0 | 0 |
| Total score | 5 | 4 | 4 | 2 | 3 | 3 | 2 | 2 | 2 | 2 | 2 | 2 | 2 | 2 | 2 | 2 | 2 | 2 |
| Irritation degree | Slight | Slight | Slight | Not | Slight | Slight | Not | Not | Not | Not | Not | Not | Not | Not | Not | Not | Not | Not |

modest degree, not significantly different between the cements. These issues tend to disappear in a longer time with bone reaction thickening around the implant. None of the cement resulted in necrotic or inflammatory reactions of relief. There were significant differences between the materials in terms of biocompatibility parameters on histological survey.

In histological preparations, the bone matrix is indicated by the presence of material fuchsin positive (f+). Histological samples of C cements did not show the presence of f+ material at any month neither in the peripheral areas nor inside the implant as shown in Figure 4 A,B,C.

Histological samples of P cement showed the presence of f+ material in the peripheral areas staring from 1st month (Figure 4D). At the 2nd month we witnessed the entry of f+ material inside the newly formed cavities in the implant; in the following months, no further progress was noticed and it remain constant until 12th month (Figure 4 E,F).

Histological samples of PG cement at the 1st month showed the presence of f+ material in the peripheral areas (Figure 5A). From the second month, we observed a progressive diffusion of f+ material over the whole sample. From the first 2 months on we observed the generation of a pattern of micro internal cavity which was rapidly invaded by organic f+ material probable of fibrinoid nature. At month 3, the cement PG showed an initial deposit of bone matrix in the peripheral portion of the sample, particularly in areas with a greater density of f+ material (Figure 5B). After 3 months it highlights the appearance, inside the plant, of cellular elongated elements of fibroblastoid morphology. In the following months, these phenomena tend to spread from peripheral areas to the entire system. At the 6th month, we observed the presence of osteoid material on the entire sample (Figure 5C, red arrows). In the built up larger blocks, you had cellular elements within gaps. The osteoid material forms within the central areas of the sample in which the fibrillar f+ material was organized to form real well cellulate connective areas (Figure 5C, yellow arrows). After the sixth month, the f+ material filled in the previous months, is flooded by fibroblastoid cellular elements likely of bone marrow origin. In fact, at the periphery of the sample is sometimes visible anatomical continuity between the internal areas of connective and bone marrow itself (Figure 5C, blue arrow). At the periphery of these connective areas, at the interface with the polymer, may yet be visible a layer of acellular fibrillar f+ material.


**Figure 2. X-rays: antero-posterior and lateral side of femurs of three treatments (C cement in top row, P cement in middle row, PG cement in the bottom row) to 1 month (left column), 6 months (middle column) and 12 months (right column). Radiographs showed good images and maintenance of the samples in the original implant areas (red circles) in all different times and for all three types of cements. Only the radiographic images of PG cement at 6 months do not show sufficiently the implant (image H). Scale bar: 1 cm.**

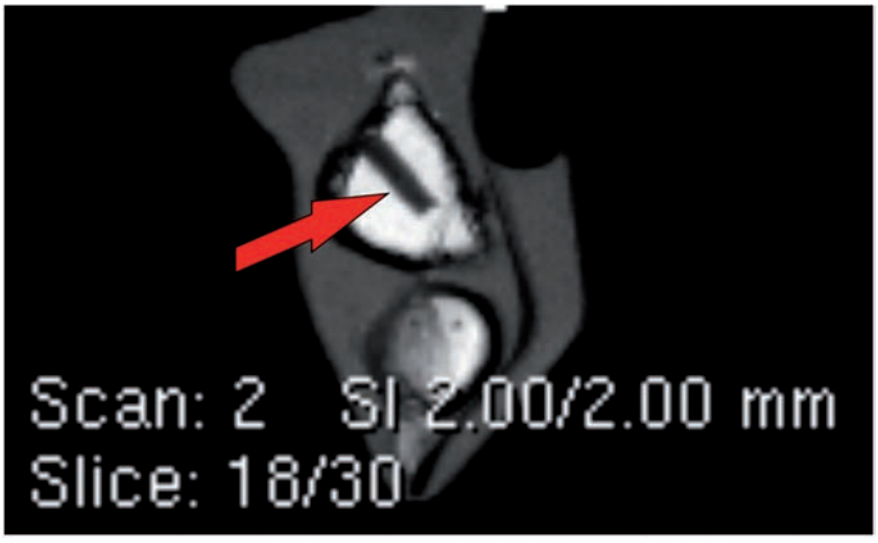


**Figure 3. MRI of PG cement at 6 months. The implant is clearly visible in its shape and position (red arrow).**

In larger areas we witnessed the deposition of bone matrix that presents isolated steps of not osteocytic gaps, and others that are organized into osteons. These areas may have a diameter <300 µm (Figure 8A, 8B, red circles). At the 9th month, the process of cavitation in the sample is very large as well as the deposition of bone matrix within the space. Indeed, also aspects of bone deposition are visible in the central portions of the sample (Figure 5D, red arrows). At the 12th month, the process of formation of bone material shall be borne by the connective interior spaces that appear in almost all sites of deposition of calcified matrix. The newly formed areas assume a morphology with osteoid formation of gaps and drafts of cellular osteons-like systems (Figure 5E, red arrows).

Results about osteointegration are reported in Figure 6. In the C cement the score was 0 at each time, showing a lack of penetration of the organic material within the polymer. The phenomena of osteointegration appears in this case due to events involving the external interface of the polymer with the tissues and bone marrow. In this regard, it was noted that the stability of the sample did not significantly alter its characteristics even in the observations carried out up to 12th month. P cement had score 1 at 1st month and score 2 at 2nd month, which remained the same till the end of the trial. The material belonging to the group P is able to generate a lattice instead of the internal micro-cavity that spreads rapidly in the whole polymer during the first two months. This lattice is rapidly invaded by organic f+ material probable of fibrinoid nature. It was noted that also in this case the remarkable stability of the pattern that does not appear to change significantly up to 12th month.

PG cement increased progressively its score from 1/2 of the 1st month up to 5 of the 12th month showing the best results between the cements. PG cement has instead shown a consistent and progressive increase of the phenomena of osteointegration.

## Ultrastructural analysis of cement with ESEM

At ESEM investigation before the implant, C cement's surface morphology shows a rare presence of pores. There is no substantial difference of the surface morphology in the samples of the C cement group from the first to the last month. It is characterized by large circular areas surrounded by widespread granular deposition. Throughout the whole samples sequence (from 1st to 12th month) there are not evidences of formation of bone matrix. The

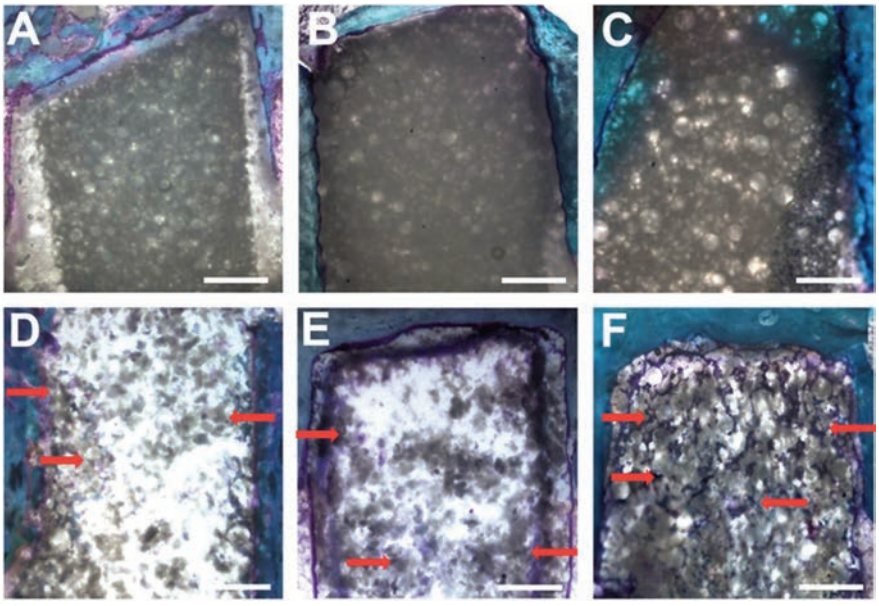


**Figure 4. Histological samples of C cement (A,B,C) and P cement (D,E,F), at 1st (A,D), 6th (B, E) and 12th month (C,F). f+ material is visible at peripheral areas of the implant (red arrows). Scale bars: 500 µm.**

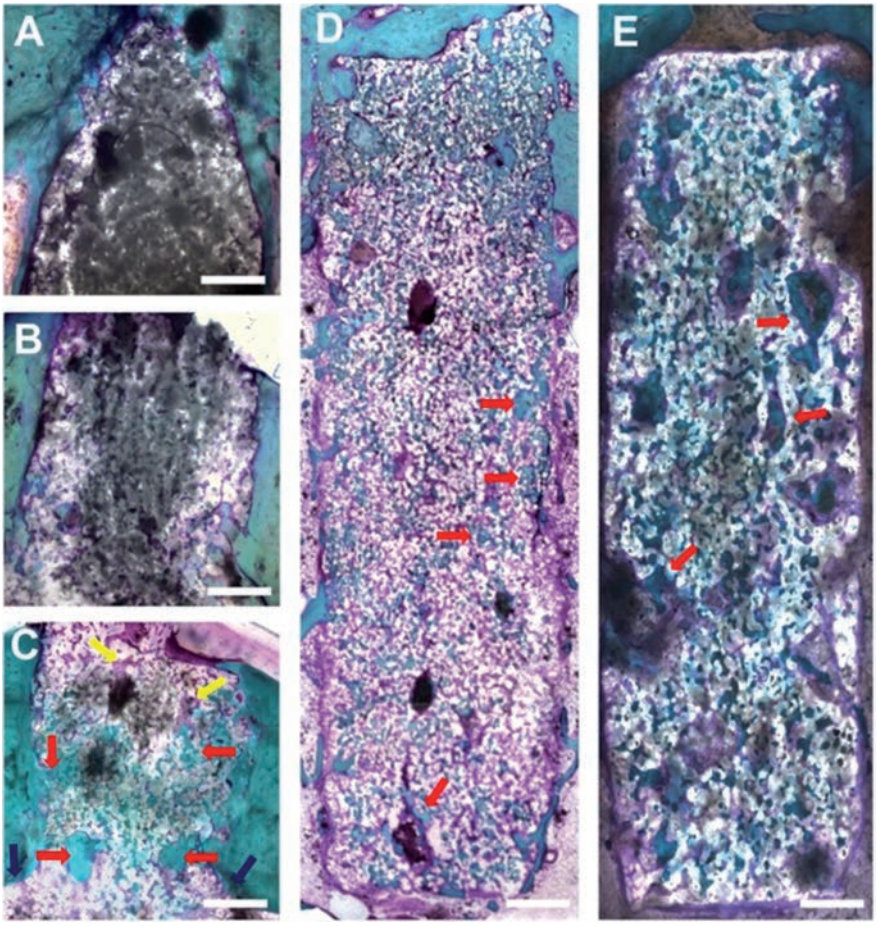


**Figure 5. Histological samples of PG cement at 1st (A), 3rd (B), 6th (C), 9th (D) and 12th month (E). f+ material is visible at peripheral areas of the implant (red arrows). Scale bars: 500 µm.**

microanalysis results are similar to the resin before the implant (Figure 7 A,B). Circular areas show main peaks attributable to carbon (C) and oxygen (O). The surrounding surfaces with granular deposition have highlighted peaks attributable to sulfur (S) and barium (Ba).

The surface morphology in the sample of P cement shows a widespread presence of 100 µm pores. From the 2nd to the 6th month, morphological analysis of P cement samples highlight some areas, inside the material, with irregular formations of deposits of granular appearance. They match with the areas weakly f+ at the histological survey. In these areas the micro analytical survey detects high peaks due to calcium (Ca) and phosphorus (P); the neighbouring area showed only peaks attributable to C and O due to the resin. On the 9th and 12th month P cement shows irregular areas with granular appearance but with low density of granules inside (Figure 8 A,B). The microanalysis shows significant peaks of Ca and P (Figure 8C). There were no relevant aspect of areas with sketches of osteons.

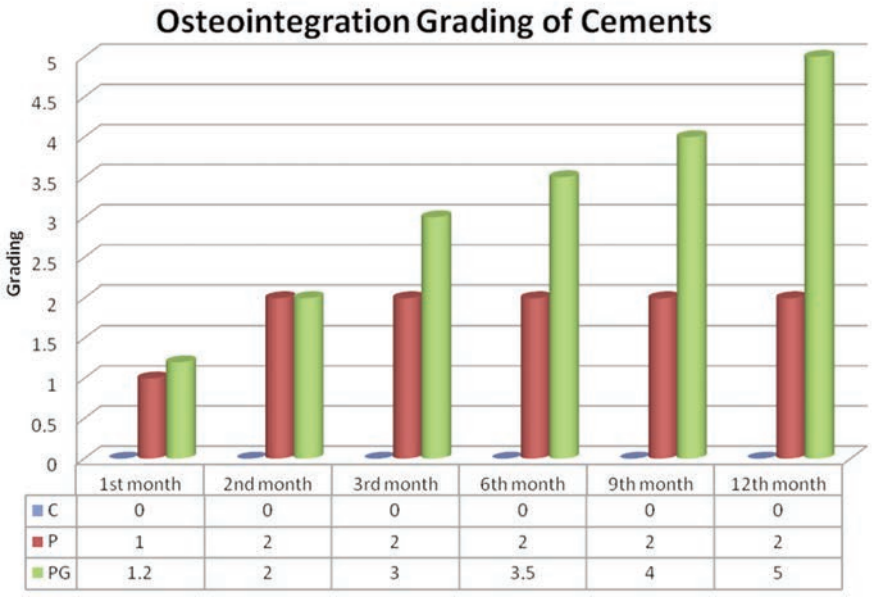


| | 1st month | 2nd month | 3rd month | 6th month | 9th month | 12th month |
|---|---|---|---|---|---|---|
| C | 0 | 0 | 0 | 0 | 0 | 0 |
| P | 1 | 2 | 2 | 2 | 2 | 2 |
| PG | 1.2 | 2 | 3 | 3.5 | 4 | 5 |

**Figure 6. Comparison of osteintegration grading at 1, 2, 3, 6, 9 and 12 months. The horizontal axis shows the time, on the ordinate the osteointegration grading.**

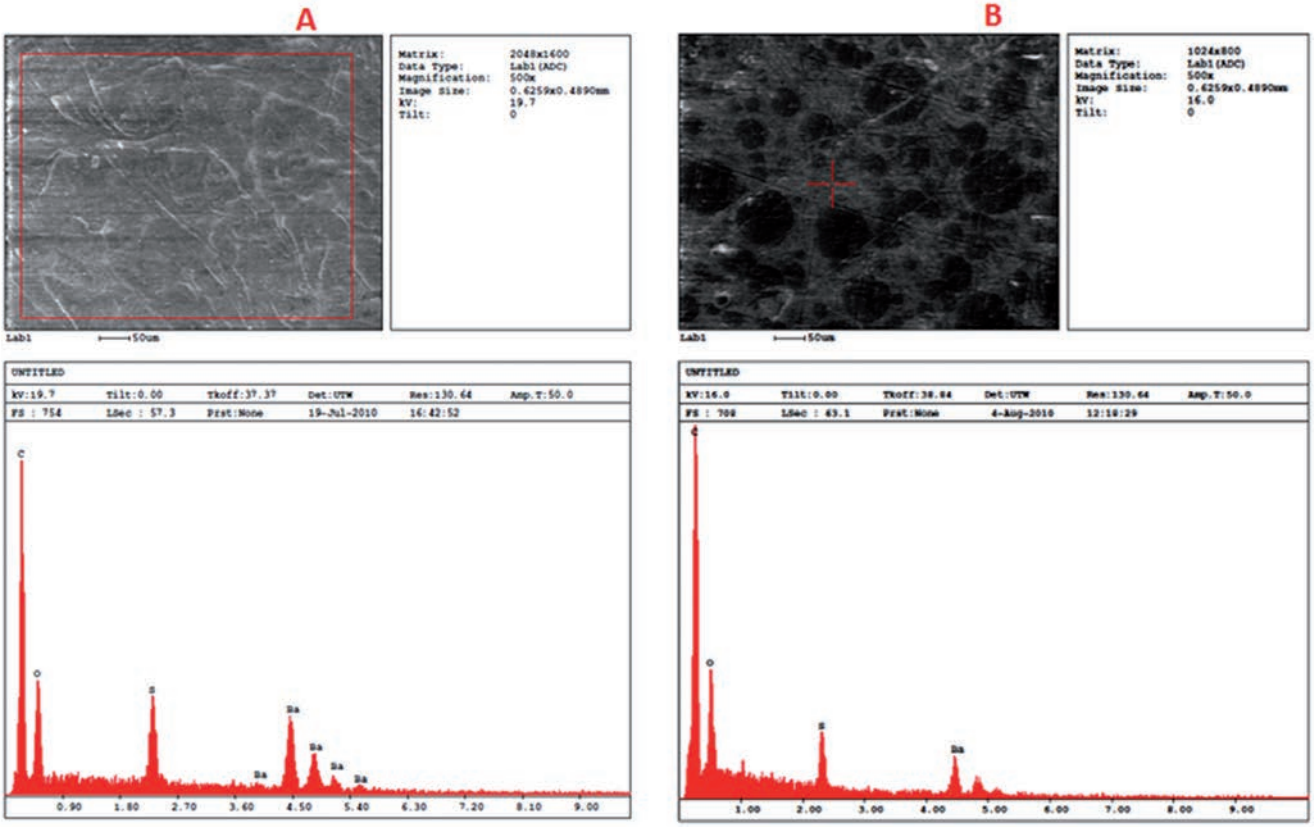


**Figure 7. C cement, ESEM microscopy of C cement cylinder before the implant (A) and at 12 months (B). The microanalysis of the sample before the implant end after 12 months shows similar peaks of C, O, S and Ba. Scale bars: A) 50 µm; B) 50 µm.**

The surface morphology in the sample of PG cement shows a widespread presence of 200-300 µm pores. Morphological analysis of PG cement inside the cylinder at 1st and 2nd month, highlighted several areas with deposits of granular appearance (Figure 9 A,B). These areas match with weakly f+ areas of histological survey. On these areas, microanalysis detected high peaks attributable to Ca and P. The neighboring areas showed peaks attributable to C and O because of its resin composition. At the 3rd month PG cement, in addition to the various areas of granular appearance, further areas begin to appear with the look of sketches of osteons (Figure 9C). These areas match with the fast green+ areas of histological survey. On all these areas, microanalytical probe detects high peaks attributable to P and Ca. Otherwise, the surrounding area showed only peaks attributable to C and O. At the 6th month, in PG cement we observed a decrease of the granular looking areas and larger number of areas of a clearer osteoid form (Figures 9D and 10 A,B). On these areas microanalytical probe detected high peaks attributable to Ca and P (Figure 10 g,o). At 9th and 12th month, in PG cement the areas with osteoid looking sketches appear to be more widespread than the granular areas which are significantly reduced. They correspond to the fast green + areas of histological survey. Such aspects are not found in adjacent areas, consist of resin alone.

## Discussion

Histological analysis showed good osteointegration of the samples. The osteointegration was mediated by the formation of a bone layer of variable thickness on the boundary of the implant. This area has no inflammatory or degenerative aspects but the newly formed tissue and appears constantly on the outside of the implanted material. Apart from this feature, we observed significant differences between the three cements. C cement has not occurred to any significant penetration of the tissues inside of the resin at any times. The others cements had significant phenomena of osteointegration not limited to the outer surface but extended within the implant. For both cements these phenomena were characterized by the penetration of a cellular matrix (f+) in the first two months of implantation. While for the P cement there have been no further developments in later times, it appears to further progress in PG cement only. In PG cement, from the third month, we witnessed a gradual onset

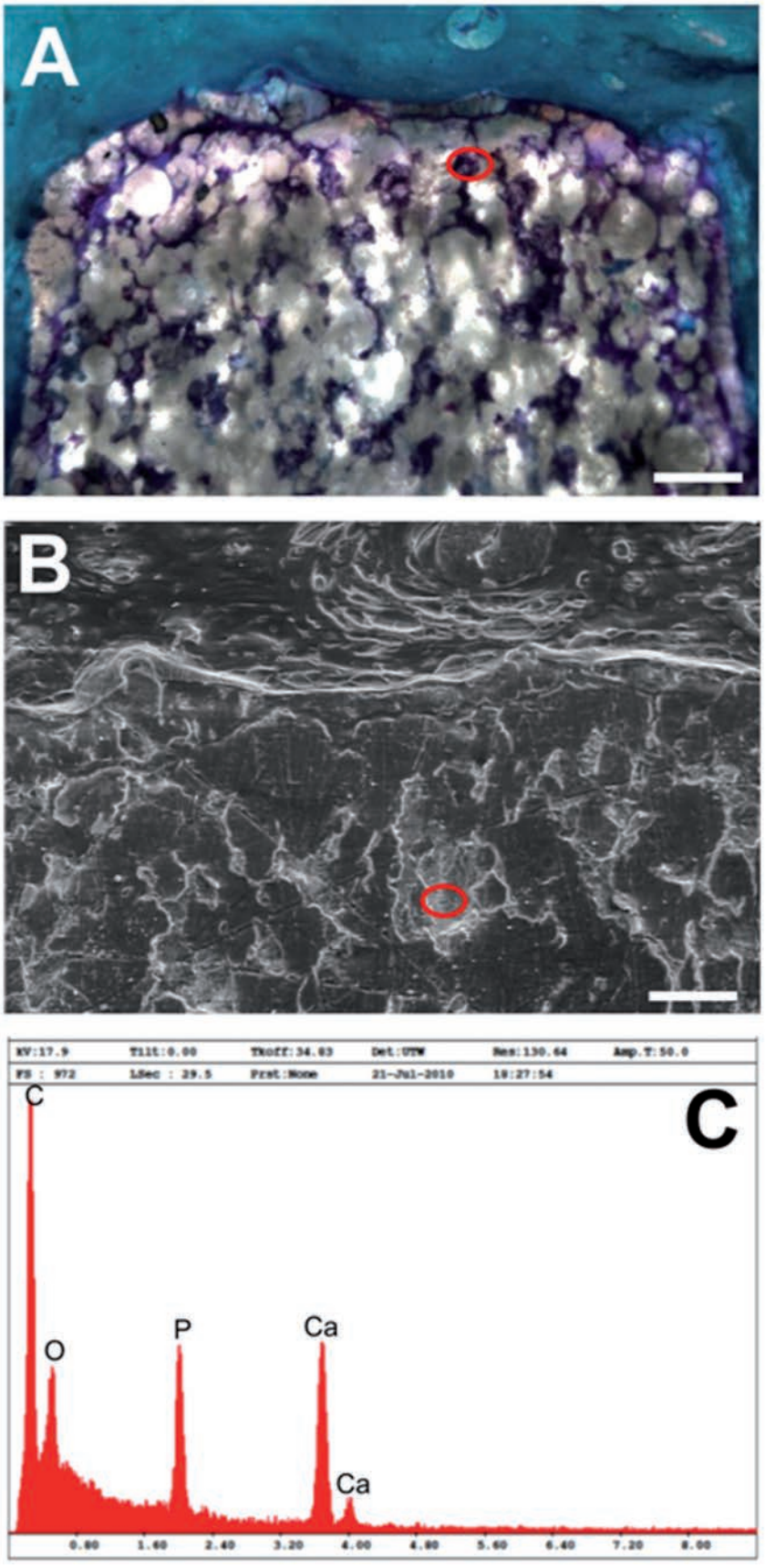


**Figure 8. P cement, optical (A) and ESEM (B) microscopy at 12 months. The microanalysis of the sample (C) shows peaks of C, O, and significant peaks of P and Ca. Scale bar: A) 200 µm; B) 100 µm.**

of cellular elements. We saw the appearance of elongated cellular elements of fibroblastoid morphology, inside the internal cavities of the implant. In the following months there is an evolution of phenomena that tend to spread from peripheral areas to the entire system. The newly formed areas progressively assume a morphology with osteoid formation of gaps and drafts of cellular osteonic-like systems. By ESEM and microanalysis we could closely follow the evolution of the three cements within a whole year of trial. As expected, in the samples of C cement from the first to the last month (1-12), we didn't observe a substantial difference of the surface morphology of the cylinder, characterized by large circular areas surrounded by areas with the presence of a widespread granular deposition. The microanalysis on the circular areas, performed in all periods, showed the main peaks attributable C and O, due to the TMMA composition and it was very similar to the microanalysis of the cylinder before the implantation. Differently, samples performed in the P cement, from the 2nd to the 12th month, show a substantial uniformity of diffusion of C and O peaks except small scattered fragments attributable to Ca and P. On 9th and 12th month, P cement showed irregular areas with granular appearance which presented significant peaks of Ca and P. However, they did not form any osteoid structure. The mapping with microanalysis of PG cement have revealed and made even more explicit the different chemical nature and morphology of the areas analyzed. From the 1st month inside the implant progressively increased several deposits of tricalcium phospate with high peaks attributable to Ca and P. At the 3rd month begin to appear sketches of osteons which become of a clearer osteoid form and greatly increase the number in the following months, replacing the granular areas. These areas were phased out by growths of bone. Because of this development PG cement, consisting of acrylic resin-based porous polymethacrylate and tricalcium phosphate has characteristics of particular interest in the process of osteointegration; especially as regards the deposition of calcified matrix within the polymer. Besides the different of barium sulphate content, the main difference between P and PG consists of the size of the granules[21,23] (granules of 53 µm only for P cement and also granules of 100-300 µm for PG cement) and pores (pores of about 100 µm for P cement and 100-200 µm for PG cement), we can assume that P cement not evolved in bone tissue inside the implant in the following months probably for the inability of the internal lattice to create the environmental conditions able to allow the evolution to the next generation of true tissue areas within the polymer.

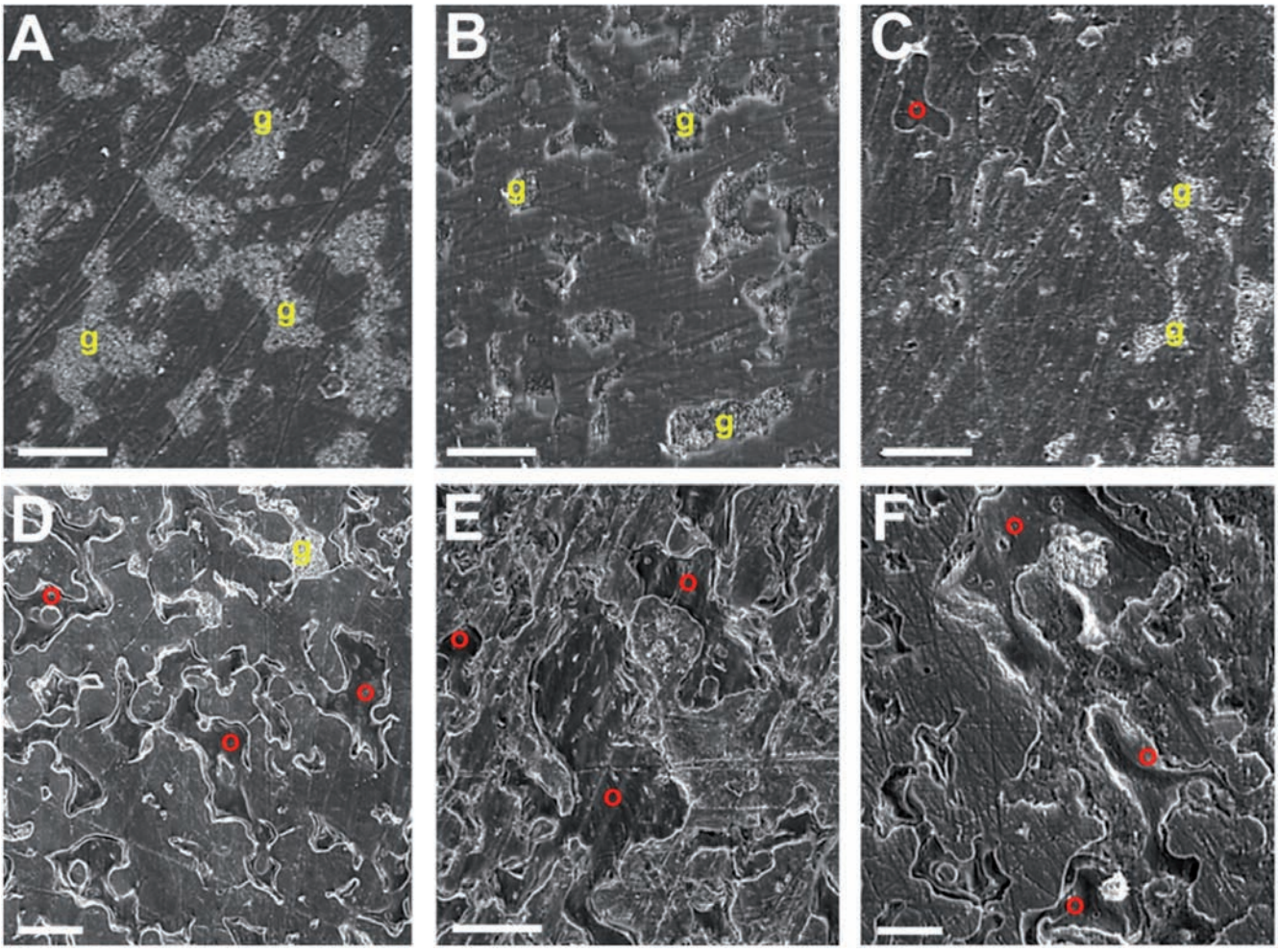


**Figure 9. PG cement, ESEM microscopy at 1, 2, 3, 6, 9, 12 months (panels A, B, C, D, E and F, respectively). The areas identified by the letters 'g' indicate the formation of granular appearance while those identified with letters 'o' indicate the osteoid formations. Scale bars: 100 µm.**

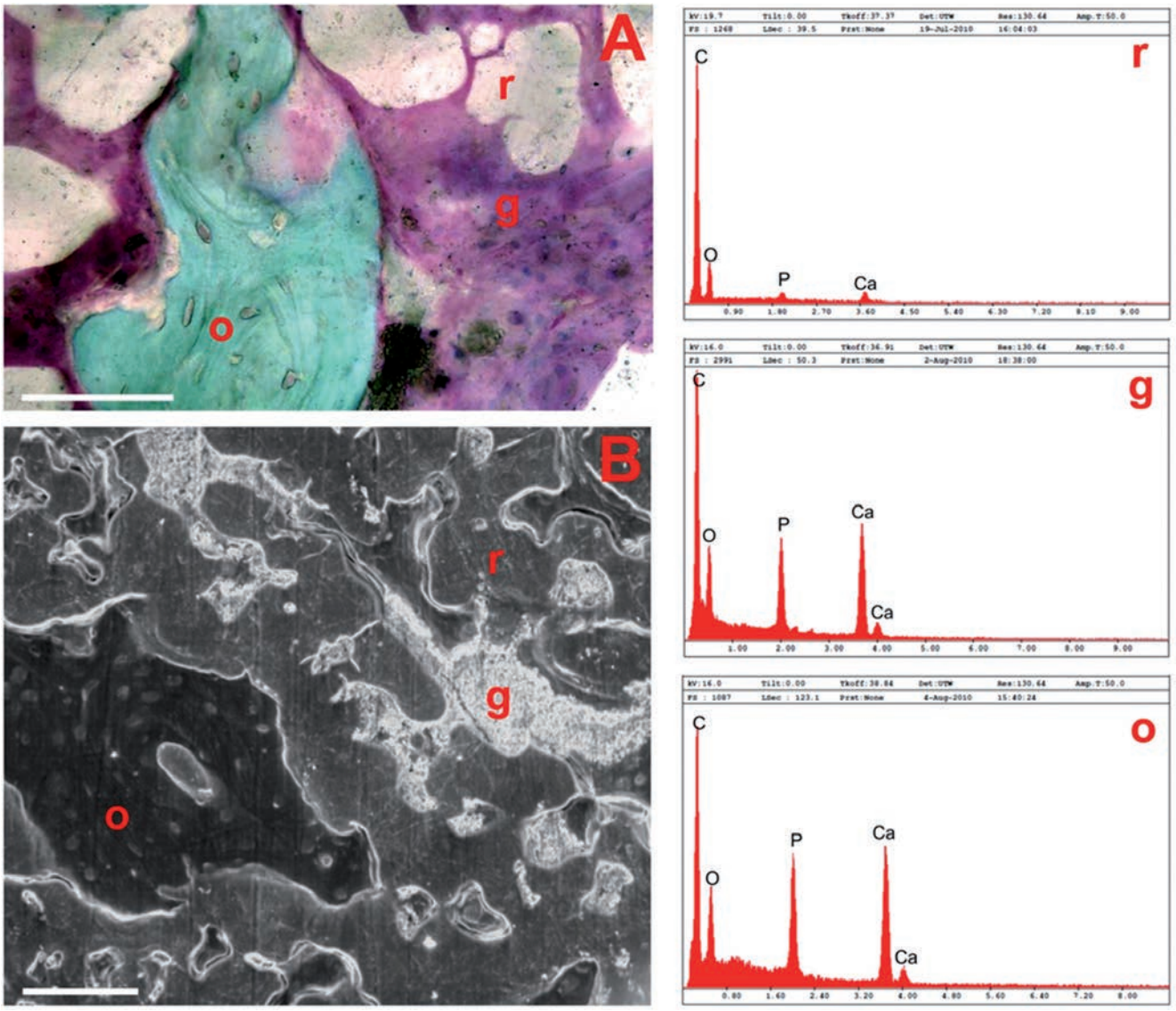


**Figure 10. PG cement, optical (A) and ESEM (B) microscopy at 6 months. The microanalysis of resin area (r) shows significant peaks of C and O and very low peaks of Ca and P. The microanalysis of granular (g) and osteoid (o) areas show significant peaks of P and Ca also. Scale bar: 100 µm.**

Hypothetically, we might assume that this non-vascular and cellular invasion is due to mechanical phenomena (pore size with insufficient access as consequence of using), rather than toxic factors, since there were no cytotoxic aspects linked to the polymer in the interface with the tissues of the host bone marrow. Granules of 100-300 µm and pores of 100-200 µm allow the penetrations of cells from the surrounding tissue creating a tridimensional scaffold that supply fluid penetration inside the matrix[17] as demonstrated *in vitro*[23] and *in vivo*[13] studies. In a previous work of Dall'Oca *et al.*[13] it was shown the importance of the use of LR white resin and the use of SEM to make complete and objective assessment of the biocompatibility of porous *vs* non porous bone cements. In this paper, we show that this evaluation process, together with the microanalysis, provides further important information that allows to follow any osteointegration at every stage of develop.

## References


1. Greewald AS, Boden SD, Goldberg VM, Khan Y, Laurencin CT, Rosier RN. Bone-Graft substitutes: facts, fictions, and applications. J Bone Joint Surg Am 2001;83:S98-103.
2. De Long WG Jr, Einhorn TA, Koval K, McKee M, Smith W, Sanders R, et al. Bone grafts and bone graft substitutes in orthopaedic trauma surgery. A critical analysis. J Bone Joint Surg Am 2007;89:649-58.
3. Giannoudis PV, Dinopoulos H, Tsiridis E. Bone substitutes: an update. Injury 2005;36:S20-7.
4. Faour O, Dimitriou R, Cousins CA, Giannoudis PV. The use of bone graft substitutes in large cancellous voids: any specific needs? Injury 2011;42:S87-90.
5. Blokhuis TJ, Arts JJ. Bioactive and osteoinductive bone graft substitutes: definitions, facts and myths. Injury 2011;42:S26-9.
6. Ebadian B, Razavi M, Soleimanpour S, Mosharraf R. Evaluation of tissue reaction to some denture-base materials: an

animal study. J Contemp Dent Pract 2008;9:67-74.
7. Webb JC, Spencer RF. The role of polymethylmethacrylate bone cement in modern orthopaedic surgery. J Bone Joint Surg Br 2007;89:851-7.
8. Moore WR, Graves SE, Bain GI. Synthetic bone graft substitutes. ANZ J Surg 2001;71:354-61.
9. Zimmermann G, Moghaddam A. Allograft bone matrix versus synthetic bone graft substitutes. Injury 2011;42:S16-21.
10. Yamada S, Heymann D, Bouler JM, Daculsi G. Osteoclastic resorption of calcium phosphate ceramics with different hydroxyapatite/β-tricalcium phosphate ratios. Biomaterials 1997;18: 1037-41.
11. Monchau F, Lefèvre A, Descamps M, Belquin-myrdycz A, Laffarque P, Hildebrand HF. In vitro studies of human and rat osteoclast activity on hydroxyapatite, beta-tricalcium phosphate, calcium carbonate. Biomol Eng 2002;19:143-52.
12. Liu B, Lun D. Current application of β-tricalcium phosphate composites in orthopaedics. Orthop Surg 2012;4:139-44.
13. Dall'Oca C, Maluta T, Cavani F, Morbioli GP, Bernardi P, Sbarbati A, et al. The biocompatibility of porous vs non-porous bone cements: A new methodological approach. Eur J Histochem 2014;58: 2255.
14. Yang HL, Zhu XS, Chen L, Chen CM, Mangham DC, Coulton LA, et al. Bone healing response to a synthetic calcium sulfate/β-tricalcium phosphate graft material in a sheep vertebral body defect model. J Biomed Mater Res B Appl Biomater 2012;100:1911-21.
15. Ge Z, Jin Z, Cao T. Manufacture of degradable polymeric scaffolds for bone regeneration. Biomed Mater 2008; 3:022001.
16. Rezwan K, Chen QZ, Blaker JJ, Boccaccini AR. Biodegradable and bioactive porous polymer/inorganic composite scaffolds for bone tissue engineering. Biomaterials 2006;27:3413-31.
17. Larsson S. Calcium phosphates: what is the evidence? J Orthop Trauma 2010; 24:S41-5.
18. Provenzano MJ, Murphy KP, Riley LH 3rd. Bone cements: review of their physiochemical and biochemical properties in percutaneous vertebroplasty. AJNR Am J Neuroradiol 2004;25:1286-90.
19. Peh WC, Gilula LA. Percutaneous vertebroplasty: indications, contraindications, and technique. Br J Radiol 2003; 76:69-75.
20. Yimin Y, Zhiwei R, Wei M, Jha R. Current status of percutaneous vertebroplasty and percutaneous kyphoplasty-a review. Med Sci Moni. 2013;19:826-36.
21. Karageorgiou V, Kaplan D. Porosity of 3D biomaterial scaffolds and osteogenesis. Biomaterials 2005;26:5474-91.
22. Von Rechenberg B, Génot OR, Nuss K, Galuppo L, Fulmer M, Jacobson E, et al. Evaluation of four biodegradable, injectable bone cements in an experimental drill hole model in sheep. Eur J Pharm Biopharm 2013;85:130-8.
23. Machado JL, Giehl IC, Nardi NB, dos Santos LA. Evaluation of scaffolds based on α-tricalcium phosphate cements for tissue engineering application. IEEE Trans Biomed Eng 2011;58:1814-9.